

## Differences in transpiration characteristics of Japanese beech trees, *Fagus crenata*, in Japan

MAKIKO TATEISHI,<sup>1,2</sup> TOMO'OMI KUMAGAI,<sup>1</sup> YOSHIHISA SUYAMA<sup>3</sup>  
and TSUTOM HIURA<sup>4</sup>

<sup>1</sup> Kasuya Research Forest, Kyushu University, Sasaguri, Fukuoka 811-2415, Japan

<sup>2</sup> Corresponding author (tmakiko@forest.kyushu-u.ac.jp)

<sup>3</sup> Field Science Center, Graduate School of Agricultural Science, Tohoku University, Naruko-onsen, Osaki, Miyagi 989-6711, Japan

<sup>4</sup> Tomakomai Research Station, Field Science Center for Northern Biosphere, Hokkaido University, Tomakomai, Hokkaido 053-0035, Japan

Received October 20, 2009; accepted February 28, 2010; published online April 14, 2010

**Summary** Japanese beech (*Fagus crenata* Blume) is widely distributed across the Japan archipelago. This species requires morphological and physiological plasticity to cope with the diverse environmental conditions across its geographical range. In this study, we monitored transpiration ( $E$ ) to examine plasticity mechanisms as an example of geographical variation in whole-tree water use. We determined  $E$  by measuring the sap flux of Japanese beech trees in three stands: Kuromatsunai (KR), Kawatabi (KW) and Shiiba (SH), which were located in different areas in Japan. We conducted biometric measurements to characterize leaf and crown morphology and evaluated geographical variations in  $E$  characteristics, such as canopy aerodynamic conductance, canopy stomatal conductance ( $G_S$ ) and decoupling coefficient ( $\Omega$ ). Leaf morphology and crown shape showed clear geographical clines. Individual leaf areas decreased in the order KR > KW > SH. The crown shape in the KR and KW stands was cylindrical but planar in the SH stand. We evaluated the effects of leaf and crown morphology on  $E$  characteristics. The  $\Omega$  values showed that, while  $E$  in the KW and SH stands was highly sensitive to  $G_S$  and atmospheric evaporative demand,  $E$  in the KR stand was sensitive to radiative energy. To maximize carbon gain without further water loss, trees maintain a high  $G_S$  in a moist habitat. For example, the KR trees may decrease  $E$  by reducing their absorbed radiation energy by adjusting the individual leaf size and crown structure. Our results indicate that the geographical variation in the water use pattern of Japanese beech is determined by the interaction between its physiological and morphological status.

**Keywords:** atmospheric, correction factor, coupling of transpiration, geographical variation, sap flow, stomatal control.

### Introduction

Tree species that grow across a wide geographic range and/or diverse habitats must cope with a variety of atmospheric and soil moisture conditions (Hacke et al. 2000, Addington et al. 2006, Poyatos et al. 2007). Genotypic variation is caused by extensive geographical distribution through natural selection resulting from environmental clines or genetic drifts and gene flows. On the other hand, phenotypic variations can involve not only genetic morphological or physiological plasticity but also non-genetic variations. That is, the phenotype can change in response to environmental variations while the genotype remains unchanged (Abrams 1994). The genotypic and phenotypic variations within each species are related to stress adaptation and ecophysiological variation, which evolve to cope with the range of environmental conditions that exist in that habitat.

Transpiration ( $E$ ) characteristics can reflect both the physiological behavior of the plant and the physical conditions of and over the canopy. The  $E$  of the tree is controlled via changes in stomatal conductance (Martin et al. 1997, Cienciala et al. 2000, Herbst et al. 2008, Kumagai et al. 2009) and through energy supply (radiation) (Wullschlegel et al. 2000, Kumagai et al. 2004, 2005). Previous studies reported that, although coniferous forest canopy is well coupled to the atmosphere, broad-leaved forest canopy is partially decoupled (e.g., Wullschlegel et al. 2000). This indicates that the  $E$  of broad-leaved forest depends on available energy received by the canopy, while the  $E$  of coniferous forest is mainly controlled by stomatal behavior. Thus,  $E$  characteristics provide basic information on energy and matter exchange between the atmosphere and vegetation. The geographical variations in  $E$ , which result from genotypic and phenotypic variations, are important for understanding the dynamics of forest ecosystems and the interactions between vegetation and atmosphere on a larger scale and in response to

climate change (e.g., Berninger 1997, Berninger and Nikinmaa 1997, DeLucia et al. 2000).

Japanese beech (*Fagus crenata* Blume) is widely distributed across the Japanese archipelago and is among the most abundant canopy tree species in Japanese cool temperate forests (see Horikawa 1972, Terazawa and Koyama 2008). Therefore, the influence of climate change on the future distribution of Japanese beech has been an important concern (e.g., Matsui et al. 2004). Japanese beech is categorized into two genotypes related to its habitat differences (ecotypes): the Pacific Ocean type (PAO) and the Japan Sea type (JAS).

Hiura (1998) reported that JAS saplings have large leaves and a conical crown, while PAO saplings have smaller leaves and a planar crown. Analysis of the variation in chloroplast DNA of Japanese beech revealed two major clades: I and II + III, which apparently correspond to the JAS and the PAO populations, respectively (Fujii et al. 2002) (see Figure 1). Although a number of field studies have reported the characteristics of matter exchange ( $\text{CO}_2$  and  $\text{H}_2\text{O}$ ) of Japanese beech at the scale of individual leaf and within a single study site (Uemura et al. 2000, 2004, 2005, Iio et al. 2005), few studies have focused on the link between variations in phenological characteristics and geographical variations (Yamazaki et al. 2007, Bayramzadeh et al. 2008).

The goal of this study, therefore, is to examine the geographical variations in  $E$  characteristics of Japanese beech

trees and to determine which factors cause such variations. Toward this goal, we have conducted tree-level measurements of xylem sap flux density ( $F_d$ ) in three Japanese beech stands across Japan over a 2-year period and compared the environmental control of whole-tree  $E$  among the stands, taking into account the morphological variations of trees (leaf size and crown shape) at each site. The outcome of this study will be useful for the development of a vegetation dynamics model that takes into account the effects of intra-specific genetic variation on growth and performance of trees (e.g., Berninger and Nikinmaa 1997).

## Materials and methods

### Study site

Japanese beech (*F. crenata*) is one of the main tree species in the Japanese cool temperate zone. It is distributed from north-eastern lowland areas on the Japan Sea side to isolated locations at small montane areas on the Pacific Ocean side in southwestern Japan. The JAS populations grow in monospecific stands, while the PAO populations form mixed stands. The experiments were carried out in three Japanese beech stands distributed across Japan. Previously, chloroplast DNA analyses (Fujii et al. 2002) suggested that Japanese beech trees at Kuromatsunai (KR;  $42^\circ 41' \text{ N}$ ,  $140^\circ 15' \text{ E}$ , 50 m a.s.l.) and Kawatabi (KW;  $38^\circ 47' \text{ N}$ ,  $140^\circ 44' \text{ E}$ , 560 m a.s.l.) belong to Clade I (JAS), while those at Shiiba (SH;  $32^\circ 22' \text{ N}$ ,  $131^\circ 10' \text{ E}$ , 1219 m a.s.l.) belong to Clade III (PAO) (Y. Suyama, unpublished data; Figure 1).

The KR stand is located at the northern limit of the distribution of Japanese beech in the Hokkaido lowlands, and the KW stand is located among the present center of its distribution at a montane area in Honshu (Field Science Center, Tohoku University). The trees at those two sites form pure Japanese beech stands. Their understory vegetation is sparse and consists mainly of *Sasa senanensis* (Franch. et Savat.) Rehd. in the KR stand and *Leucothoe grayana* Maxim. in the KW stand. There are a few individuals of *Quercus crispula* Blume and *Acer japonicum* Thunb. at the KW site. The SH stand is located at a montane area in Kyushu Island (Shiiba Research Forest, Kyushu University). Trees at this site form a mixed stand with other species. The canopy at SH is dominated by Japanese beech, *Abies firma* Sieb. et Zucc., *Q. crispula* and *Acer sieboldianum* Miq. The sub-canopy species consist of *Pieris japonica* (Thunb.) D. Don. and *Symplocos myrtaea* Sieb. et Zucc. The stem basal area of the Japanese beech trees at the KR, KW and SH stands were 56.6, 32.2 and 34.7  $\text{cm}^2 \text{ m}^{-2}$ , respectively, measured in a 100- $\text{m}^2$  plot at each stand.

The bedrock at the three sites is the Neogene sediment, which comprised two different main members: pyroclastic stone and silt and sandstone at KR, the Tertiary tuff with volcanic ash at KW and schistose sandstone and phyllite at SH. The climate of the KR and the KW stands is typical

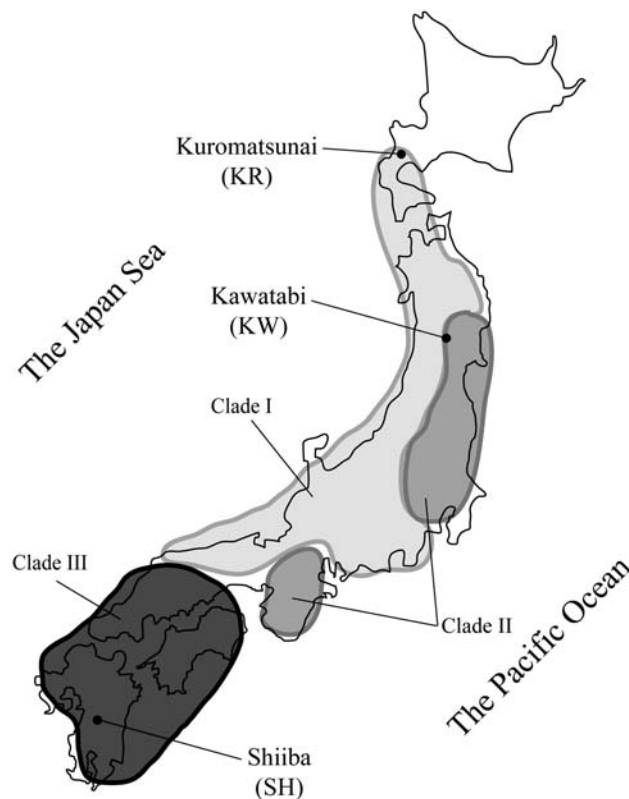


Figure 1. Geographical distribution of three clades of Japanese beech determined from chloroplast DNA analysis and location of study sites (figure redrawn from Fujii et al. 2002).

Table 1. Characteristics of 12 trees used for sap flux measurements and number and positions of sensors at the three study sites: Kuromatsunai (KR), Kawatabi (KW) and Shiiba (SH). DBH, diameter at breast height;  $l$ , crown depth;  $d$ , crown diameter; LAI, leaf area index.

Site	Tree no.	DBH (cm)	Height (m)	$l$ (m)	$d$ (m)	LAI <sup>1</sup>	Numbers of fixed sensors at depths		
							0–20 mm	20–40 mm	40–60 mm
KR	1	42.3	19.7	15.2	9.6	6.9	2	2	2
	2	29.7	18.7	17.1	5.4	9.6	2	2	2
	3	28.0	20.2	8.6	5.7	7.5	2	2	2
	4	17.4	20.0	11.7	3.5	6.5	2	1	–
KW	1	38.3	21.5	13.7	6.5	4.9	2	2	2
	2	29.3	20.8	12.3	6.5	3.2	2	2	2
	3	28.5	21.0	14.4	5.6	4.1	2	2	2
	4	17.6	19.7	16.8	4.5	2.7	2	1	–
SH	1	40.2	16.0	10.2	10.7	4.1	3	2	2
	2	39.6	16.5	13.9	11.8	3.3	3	2	2
	3	17.7	15.0	9.2	5.6	2.2	2	2	2
	4	13.3	12.5	5.3	4.0	2.2	2	1	1

<sup>1</sup>LAI was estimated as the value of total leaf area divided by projected crown area of each study tree.

of the Japan Sea side of the Japanese archipelago and is characterized by heavy snowfall, while there is little snowfall at the SH stand (Japan Meteorological Agency 2010). The mean annual air temperature ( $T_a$ ) in the KR stand was 7.2 °C, with mean January and August  $T_a$  of –4.6 and 20.5 °C, respectively. In the KW stand, the mean annual  $T_a$  was 10.2 °C, with mean January and August  $T_a$  of –1.1 and 22.4 °C, respectively (Japan Meteorological Agency 1979–2006). At the SH stand, the mean annual  $T_a$  was 12.9 °C, with mean January and July  $T_a$  of 2.5 and 22.9 °C, respectively (Kyushu University Forests 2000–06). Mean annual precipitation was 1446, 1650 and 2790 mm at the KR, KW (1979–2006) and SH (2000–06) stands, respectively.

#### Sap flux measurements

$F_d$  measurements were conducted using the thermal dissipation method with Granier-type sensors (e.g., Granier 1987). Each sensor consists of two probes: one upper and one lower. The probes were inserted into the sapwood ~0.15 m apart. The upper probe, which includes a heater, was supplied with 0.2 W constant power. The heat was dissipated into the sapwood and vertical sap flux surrounding the probe. The temperature difference between the upper heated probe and lower unheated reference probe was then measured and converted to  $F_d$  according to Granier (1987). Here, we defined the highest temperature difference ( $\Delta T_{\max}$ ) as the zero flux condition for each day. The  $\Delta T_{\max}$  values determined each day were similar throughout the study period. Sap flow signals were recorded on a data logger (CR1000; Campbell Scientific, Logan, UT) with a multiplexer (AM16/32; Campbell Scientific) every 30 s and were averaged over 30 min.

It is difficult to visually identify the boundary between sapwood and heartwood in Japanese beech trees (see Kubota et al. 2005). Thus, we used two types of sensor, a fixed sensor and a mobile sensor, to determine the hydroactive area and the spatial variation in  $F_d$  in the stem cross-sectional area.

The fixed sensor comprised a pair of probes 20 mm long and 2 mm in diameter. The upper probes contain a thermocouple conjunction and a heater and the lower probe contained a thermocouple conjunction. The mobile sensor used in this study was designed as described by Delzon et al. (2004). The upper and lower probes were installed into the stem in previously inserted long aluminium tubes to examine the coverage of the hydroactive area.

For  $F_d$  measurements, four trees were selected at each site, so that the range of diameter at breast height (DBH) overlapped among the sites (Table 1). To investigate the radial and azimuthal variations in  $F_d$ , three to six sensors were inserted into each selected tree at several depths and directions. Table 1 shows the numbers of sensors installed for examining the azimuthal variation at one depth. First, the 0–20-mm sensors were placed at the given directions around each tree, and then, the other depth sensors were placed ~10 cm apart vertically and circumferentially at proximate sensors at 0.8–1.3 m height. In addition, the mobile sensors were used to measure  $F_d$  at four (~60–80 mm) to six (~100–120 mm) depths in each of the study trees, and the deepest position was defined as the position where an  $F_d$  value <10% of  $F_d$  at 0–20 mm was observed. The part of the trunk where the sensors were inserted was fully insulated from the ground to avoid ‘morning peaks’ caused by direct radiation and thermal gradients along the trunk (see Lu et al. 2004).

For the investigations in this study, we used continuous  $F_d$  data obtained in the 2007 growing season during the 2-year observation period. Also, intensive observations using the mobile sensors were conducted for more than 24 h for each measurement depth from August to October 2007.

#### Leaf area and crown shape measurements

The total leaf mass of each sample tree ( $M_L$ ) was obtained using a  $M_L$ –DBH allometry equation:  $\ln(M_L) = p + q \ln(\text{DBH})$  (where  $p$  and  $q$  are the parameters and  $M_L$  and DBH

are represented in g and cm, respectively) for Japanese beech. Hiura (1998) reported that the allometry parameters are specific for PAO and JAS populations. Thus, we used the allometry parameters from Oshima peninsula ( $p = 1.203$ ,  $q = 2.35$ ; T. Hiura, unpublished data;  $41^{\circ}45' \text{ N}$ ,  $140^{\circ}08' \text{ E}$ ) and Niigata ( $p = 2.87$ ,  $q = 1.7$ ; Hiura 1998;  $37^{\circ}35' \text{ N}$ ,  $139^{\circ}11' \text{ E}$ ) to calculate  $M_L$  of trees in the KR and KW stands, respectively, selecting the reference sites nearest to our study sites. Since there is no allometric data for Japanese beech in Kyushu Island in southern Japan, we used previously obtained allometric data for smaller trees (T. Hiura, unpublished data) and harvested four larger trees destructively in the SH stand in August 2008 ( $p = 1.404$ ,  $q = 2.38$ ).

Three 0.5-m<sup>2</sup> circular litter traps were positioned 1 m above the ground in the 100-m<sup>2</sup> plot at each site. From May to November, abscised leaves were collected monthly and were identified as Japanese beech leaves. These sample leaves were dried for at least 72 h at 60 °C, and dry mass and leaf areas of a subsample of 50 leaves from each litter trap were obtained to determine the specific leaf area (SLA; m<sup>2</sup> kg<sup>-1</sup>). The total leaf area of each sample tree ( $A_L$ ) was then obtained by multiplying SLA by  $M_L$  for that tree. In addition, the total dry mass of leaves from three litter traps at each site was used to compare and confirm the difference in  $A_L$  of sample trees among the three sites.

Crown depth ( $l$ ; m) and diameter ( $d$ ; m) were determined by subtracting the height at the base of the live crown from the tree height and by the geometric means of the north–south and east–west widths of the projected crown, respectively. The ratio,  $d/l$ , represents the crown shape of the sample tree: the value is higher when the crown shape is planar and lower when the crown shape is cylindrical. The leaf area index (LAI) of each sample tree was calculated by dividing its  $A_L$  by the projected crown area.

#### Meteorological measurements

We measured meteorological conditions with a solar radiometer (LP PYRA 03; Delta Ohm, Padua, Italy), a temperature and relative humidity sensor (HMP45A; Vaisala, Helsinki, Finland) and a wind speed and direction meter (Model 05305; R.M. Young, Traverse City, MI). These instruments were installed at the top of a scaffold tower at each site (20–23 m height), except at the KR site where the solar radiometer was placed at an open space within 50 m of the tower. Samples were taken every 5 s and averaged over 10 min (CR1000). The net radiation above the canopy ( $R_n$ ; W m<sup>-2</sup>) was not measured but was derived from the measured solar radiation ( $R_s$ ; W m<sup>-2</sup>) using the relationship  $R_n = 0.84R_s - 15.21$  ( $R^2 = 0.99$ ), which was obtained from measurements from a net radiometer (CNR1; Kipp & Zonen, Delft, The Netherlands) conducted at the SH stand from July to August 2008.

Volumetric soil moisture content ( $\theta$ ) and matric potential ( $\psi$ ) were measured in each site at 0.1, 0.2 and 0.4 m below the forest floor at 1-h intervals (CR1000). A dielectric aqua-

meter sensor (EC-10; Decagon Devices, Inc., Pullman, WA) was used to measure the time series of  $\theta$ . A tensiometer (Special Order, Environmental Measurement Japan Co. Ltd, Fukuoka, Japan) was used to monitor  $\psi$  at the same depth as  $\theta$ , thereby providing the necessary measurements to calculate in situ  $\theta$ – $\psi$  curves, i.e., soil water retention curves.

#### Calculations of whole-tree transpiration and canopy stomatal conductance

To obtain the representative  $F_d$  at each sensor depth,  $i$ , ( $F_{di}$ ), we averaged several values of  $F_d$  at the same depth, including the  $F_d$  from the mobile sensor, for each sample tree (see Table 1). To extrapolate  $F_d$  from the outer 20 mm of the xylem ( $F_{dref}$ ) to the entire sapwood area, we calculated a correction coefficient ( $C$ ) that accounts for both the radial  $F_d$  profile and the area of the xylem band ( $A_i$ ) sampled at each depth (Delzon et al. 2004):

$$C = \sum_{i=1}^N v_i \frac{A_i}{A_S} \quad (1)$$

in which:

$$v_i = \frac{\overline{F_{di}}}{F_{dref}} \quad (2)$$

where  $N$  is the total number of depths measured in the xylem and  $A_S$  is the entire cross-conducting area. The overbar denotes an ensemble average over the selected data when  $R_s > 400 \text{ W m}^{-2}$ . Note that  $v_i$  can vary between 0 and 1 ( $v_1$ , at 0–20 mm).

If there is a capacitive exchange between the  $E$  stream and the stem water storage, there is a significant time lag between  $F_d$  measured at the base of the stem and  $E$  (Phillips et al. 1997, Kumagai 2001, Meinzer et al. 2003, Ford et al. 2005, Kumagai et al. 2009). Thus, we examined the lag between  $F_{dref}$  and the above-canopy atmospheric humidity deficit ( $D$ ; Pa) using cross-correlation analysis of their time series and confirmed that  $F_{dref}$  did not lag  $D$ . Therefore, whole-tree  $E$  ( $E_T$ ) was calculated from the  $F_{dref}$  as follows:

$$E_T = F_{dref} \times A_S \times C. \quad (3)$$

Also, we calculated  $E_T$  per unit leaf area ( $E_L$ ) as  $E_T/A_L$ . Using  $E_L$  and some meteorological variables, canopy stomatal conductance ( $G_S$ ; m s<sup>-1</sup>, mean canopy stomatal conductance per unit leaf area: see Pataki and Oren 2003) was calculated with the inverted Penman–Monteith equation:

$$G_S = \frac{\gamma \lambda E_L G_a}{\Delta (R_{abs}/LAI) + \rho_a c_p G_a D - \lambda E_L (\Delta + \gamma)} \quad (4)$$

where  $\gamma$  is the psychrometric constant (66.5 Pa K<sup>-1</sup>),  $\lambda$  is the latent heat of vaporization of water (J kg<sup>-1</sup>),  $G_a$  is the mean canopy aerodynamic conductance (m s<sup>-1</sup>),  $\Delta$  is the rate of change of saturation water vapour pressure with temperature

(Pa K<sup>-1</sup>),  $R_{\text{abs}}$  is the net radiation absorbed by each tree (W m<sup>-2</sup>),  $\rho_a$  is the density of dry air (kg m<sup>-3</sup>) and  $c_p$  is the specific heat of air at constant pressure (J kg<sup>-1</sup> K<sup>-1</sup>).

In Eq. (4), we used  $R_{\text{abs}}$  to estimate available energy for a tree crown, instead of the difference between  $R_n$  and soil heat flux, which is the standard method for the Penman–Monteith equation.  $R_{\text{abs}}$  was calculated as in Granier and Loustau (1994), as follows:

$$R_{\text{abs}} = R_n [1 - \exp(-k\text{LAI})] \quad (5)$$

where  $k$  is the Beer's law extinction coefficient.  $G_a$  results from the series sum of leaf boundary layer conductance ( $g_b$ ) and turbulent conductance ( $g_t$ ) as in Choudhury and Monteith (1988), Köstner et al. (1992) and Magnani et al. (1998), as follows:

$$G_a^{-1} = g_b^{-1} + g_t^{-1} \quad (6)$$

in which:

$$g_b = b \sqrt{\frac{u[1 - \exp(-\alpha/2)]}{d_m \alpha}}, \quad (7)$$

$$g_t = \frac{\kappa^2 u}{\text{LAI} \{ \ln[(z-d)/z_0] \}^2} \quad (8)$$

where  $b$  is a proportionality coefficient ( $3.62 \times 10^{-3}$ ; see Campbell and Norman 1998),  $u$  is the wind speed at the top of the canopy (m s<sup>-1</sup>),  $\alpha$  is an attenuation coefficient for wind speed inside the canopy (3.0),  $d_m$  is the characteristic dimension (m) calculated as the square root of a leaf area,  $\kappa$  is the von Karman constant (0.4),  $z$  is the canopy height (m) and  $d$  and  $z_0$  are the zero-plane displacement (m) and roughness length (m) respectively, set as 2/3 and 1/10 of the canopy height, respectively.

To evaluate the sensitivity of  $E$  to stomatal control, the decoupling coefficient,  $\Omega$ , was calculated according to Jarvis and McNaughton (1986), as follows:

$$\Omega = \frac{\Delta/\gamma + 1}{\Delta/\gamma + 1 + G_a/G_s}. \quad (9)$$

$\Omega$  is a measure of the coupling between conditions at the surface and in the free airstream and varies between 0 (for perfect coupling) and 1 (for complete isolation); stomatal control of  $E$  grows progressively weaker as  $\Omega$  approaches 1 (see Jones 1992).

Analyses were conducted from July to October (mid-growing season) in 2007 because of the ideal environmental conditions. During that period, there were appreciable day-to-day variations in radiation, temperature and humidity with moist soil conditions. The soil conditions were relatively dry in the KR stand in late August, but we confirmed this had little effect on  $E$  of beech trees.  $F_d$  values obtained during rain events were discarded.

## Results and discussion

### Morphological characteristics of individual leaf and crown

The phenotype of Japanese beech trees gradually changes over its geographical range, i.e., there is a geographical cline in leaf size. The leaf size gradually increases from southwestern to northeastern populations (Hagiwara 1977). In addition, Tomaru et al. (1997) and Hiura (1998) suggested that the PAO populations have smaller leaves than the JAS populations. Also, Hiura (1998) and Koike and Maruyama (1998) observed that the SLAs of saplings in the PAO populations were smaller than those of saplings in the JAS populations. Our results were consistent with these previous reports, in that both the SLA and individual leaf area of canopy trees decreased in the following order: KR > KW > SH (Figure 2).

As Hiura (1998) pointed out, such a geographical cline might be explained by optimal leaf size theory for photosynthesis under light-moisture conditions (e.g., Parkhurst and Loucks 1972). In fact, compared with leaves of PAO saplings, leaves of JAS saplings were larger and thinner, had only one layer of palisade tissue, had a smaller air space ratio and had a lower area-based photosynthetic rate (Koike and Maruyama 1998). Similar differences were observed between sun and shade leaves of European beech trees, and this

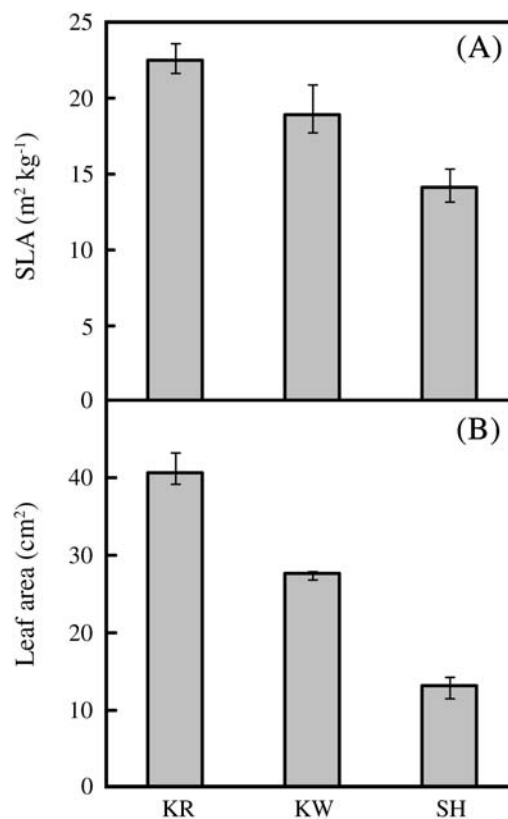


Figure 2. Leaf structural characteristics, (A) SLA and (B) leaf area, of Japanese beech trees from three stands: KR, KW and SH (see Figure 1). Top and bottom of vertical bars indicate maximum and minimum, respectively ( $n = 3$ ).

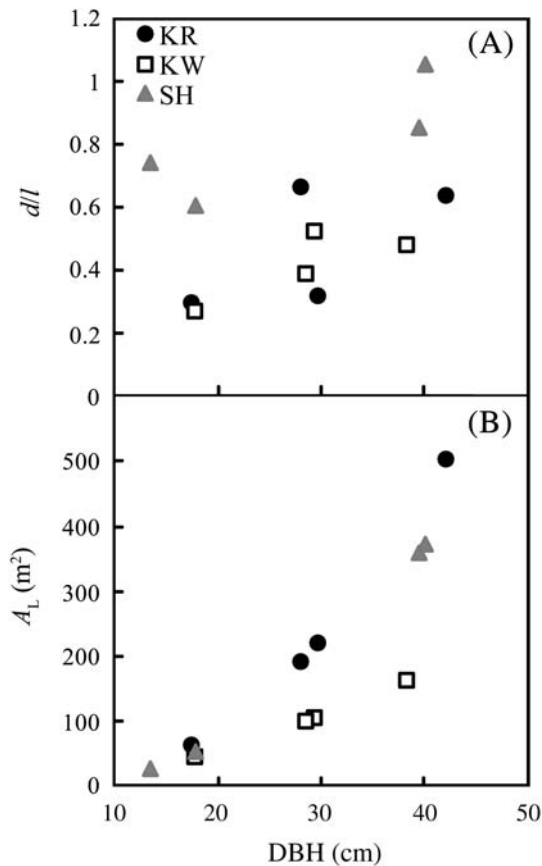


Figure 3. Relationships between DBH and crown shape parameter  $d/l$  (where  $d$  and  $l$  are crown depth and diameter, respectively) (A) and total leaf area ( $A_L$ ) (B) of each sample tree in KR, KW and SH stands.

was thought to be related to light conditions (Kutsch et al. 2001). Phenotypic variations among Japanese beech populations may also result from stress adaptation at each site. For example, compared with sites facing the Japan Sea, sites facing the Pacific Ocean are generally drier and have continual higher light conditions (see Koike and Maruyama 1998).

Figure 3A compares crown shapes and their relationship to the tree size (DBH) for the three sites. Trees in the SH stand showed more depressed crown shapes than those in the KR and KW stands. This result was consistent with the previous observation that large-leaf Japanese beech trees tend to form cylindrical canopies, while small-leaf Japanese beech trees tend to form planar canopies (Hiura 1996). On average, the crown shapes of the sample trees at all study sites became more depressed as the DBH increased (Figure 3A). Crown shapes of trees at high-latitude regions tend to be more upright and cylindrical in form, compared with those at low latitudes. This is mainly attributed to lower annual solar elevation (e.g., Kuuluvainen 1992). Hiura (1998) suggests that such crown shapes of trees are genetically determined by shoot mortality caused by their leaf size, i.e., the optimal growth of their genotypes.

On the other hand, there was no geographical cline in the relationship between DBH and  $A_L$  (Figure 3B). As calculated

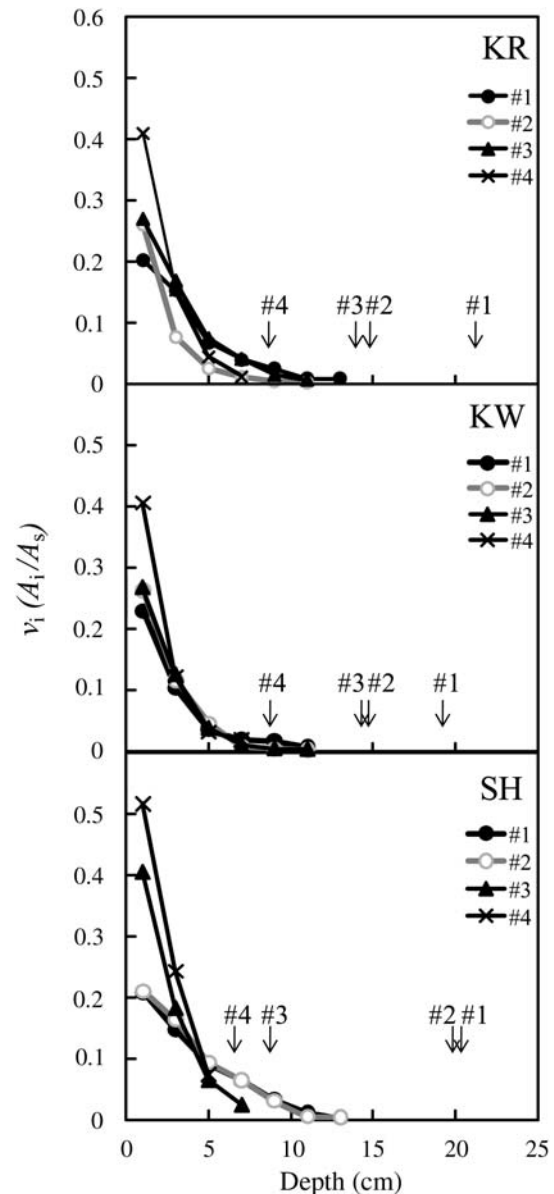


Figure 4. Radial profile of area-weighted sap flow ratio ( $v_i(A_i/A_s)$ ; see Eq. (1)) as a function of depth in the stems of sample trees #1–4 in KR, KW and SH stands. Arrows indicates depth of pith in the stem of each sample tree.

using DBH– $A_L$  allometric curves, the  $A_L$  values at the same DBH, e.g., around 40 cm, were similar in the trees in the KR and SH stands, while those in the KW stand were lower. It should be noted that the cylindrical crown shape and larger  $A_L$  of trees in the KR stand resulted in appreciably higher LAI values than those in the KW and SH stands (Table 1).

#### Radial variations in sap flux and correction factors

Figure 4 shows the radial variations in the area-weighted sap flow ratio ( $v_i(A_i/A_s)$ ), a term in Eq. (1), in the stems of all sample trees at each study site. Almost all of the stem xylem in smaller trees conducts water (see Lu et al. 2000, Hirose et

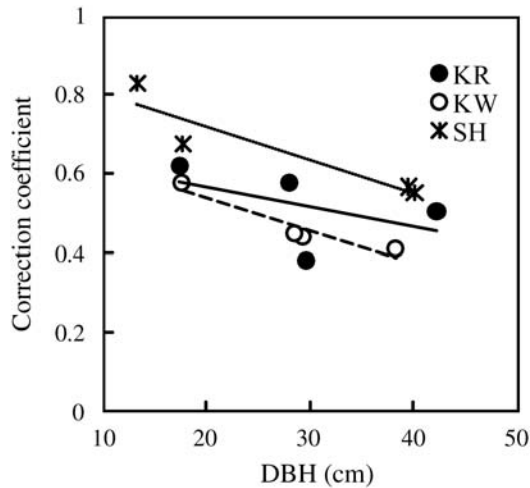


Figure 5. Relationship between correction coefficient (see Eq. (1)) and DBH for each sample tree in KR, KW and SH stands. Lines denote linear regressions for data from KR (solid line), KW (broken line) and SH (dotted line) stands.

al. 2005, Tateishi et al. 2008). On the other hand, the depth of the hydroactive zone in the stem of the largest tree (DBH  $\approx$  40 cm) in each study site was around 12 cm. This result sug-

gested that the ratio of hydroactive area to non-conducting area became smaller as the stem diameter increased, regardless of the study site. Our experiments using dye solution confirmed these relationships between tree size and the depth of conducting sapwood (Y. Utsumi, unpublished data). Furthermore, Figure 4 illustrated that both the larger hydroactive area and the higher  $F_d$  close to the bark explain the greater contribution of the outer xylem to the whole-tree  $E$  (e.g., Delzon et al. 2004). At all study sites, the ratio,  $v_i(A_i/A_S)$ , was higher in smaller trees (DBH < around 20 cm) than in larger trees, and the  $v_i(A_i/A_S)$  decreased more sharply with increasing stem depth in smaller trees than in larger trees.

This result implies that the  $v_i(A_i/A_S)$  of large trees at deeper depths gives a somewhat significant contribution to their correction coefficient ( $C$ ; Eq. (1)) despite their smaller ratio of sapwood to the entire stem section. Unlike Delzon et al. (2004), we did not find a clear relationship between  $C$  and DBH at each study site (Figure 5), and the slopes of the linear regression were not significantly different from zero ( $P = 0.53, 0.06$  and  $0.08$  for KR, KW and SH, respectively). On the other hand, the mean value of  $C$  in the SH stand was significantly higher than those in the KR and KW stands, and

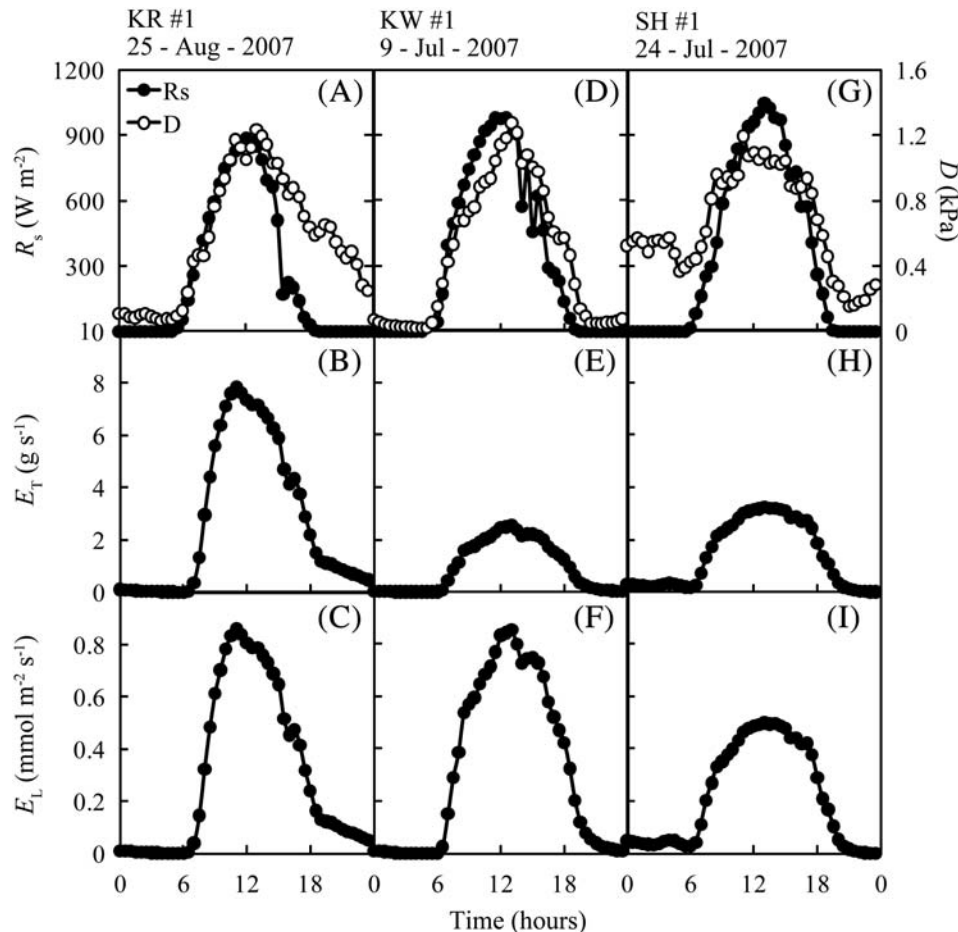


Figure 6. Diurnal pattern of solar radiation (A, D, G) ( $R_s$ ), atmospheric humidity deficit ( $D$ ), whole-tree transpiration (B, E, H) ( $E_T$ ) and transpiration per unit leaf area (C, F, I) ( $E_L$ ) for tree #1 in the KR stand (A–C), tree #1 in the KW stand (D–F) and tree #1 in the SH stand (G–I).

there was no significant difference between  $C$  values of the KR and KW stands ( $P < 0.05$ ). Although this result suggests, when assuming the same tree size, the higher effectiveness for water transportation in hydroactive sapwood in SH compared with KR and KW, even the value of  $C$  in SH was much less than the  $C$  reported in previous studies (at least, around 0.8; Köstner et al. 1996, Zang et al. 1996, Wullschlegel and King 2000, Delzon et al. 2004). Thus, it is logical to assume that the  $C$  of sample trees was independent of the differences in the tree size (DBH) and the study site.

The whole-tree  $E$  of trees in the KR, KW and SH stands was calculated using the  $C$  estimated for each study site. The characteristics are discussed in the following sections.

#### Transpiration characteristics

We compared diurnal patterns of  $E_T$  and  $E_L$  among trees in the KR, KW and SH stands (Figure 6). For these analyses, we selected trees of similar size and growing under similar environmental conditions. The  $E_T$  was much higher in trees

in the KR stand, while the  $E_L$  values for the KR and KW trees were very similar. These findings illustrate that the effective hydraulic architecture in SH trees did not affect their efficiency of leaf-scale gas exchange, i.e.,  $G_S$ , and that the difference in whole-tree water use between KR and KW was determined mainly by  $A_L$  rather than  $G_S$  (Figures 5 and 6C, F, I).

Figure 7 further compares transpiration characteristics ( $G_a$ ,  $G_S$  and  $\Omega$ ) among trees at the three stands. These values were calculated from average  $F_d$  measurements around noon (1100–1300 LT). We compared transpiration characteristics among trees at each site and the averaged values among the three sites. Hereafter,  $G_a$  and  $G_S$  refer to midday values and  $\Omega$  refers to the decoupling coefficient calculated using these midday values. Note that, on average, the midday value, especially  $G_S$ , represents the most favourable (maximum) stomatal opening. Thus, the midday value is a relatively straightforward estimate of the maximum value. The values of  $G_S$  and  $\Omega$  must be affected by the canopy extinction coefficient,  $k$ , which varies according to canopy architecture, such as leaf distribution and angle (Eqs. (4) and (5); see

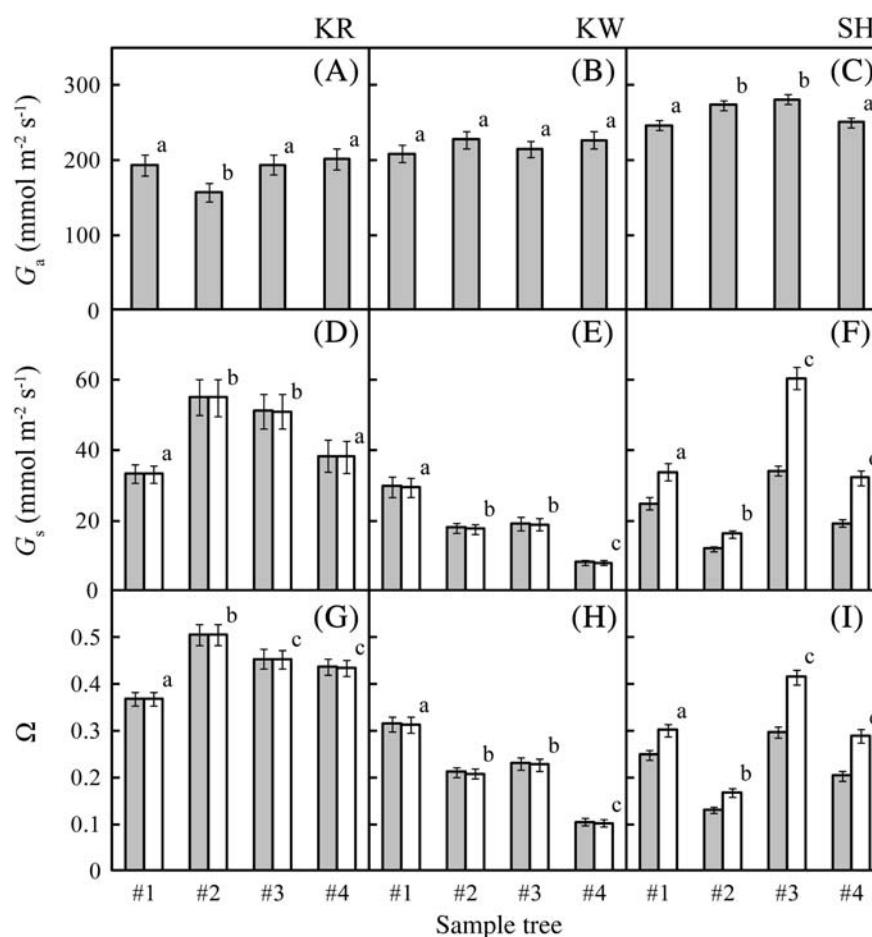


Figure 7. Mean canopy aerodynamic conductance (A–C) ( $G_a$ ), mean canopy stomatal conductance (D–F) ( $G_s$ ) and decoupling coefficient (G–I) ( $\Omega$ ) for each sample tree in the KR (A, D, G), KW (B, E, H) and SH (C, F, I) stands. Values are averaged over the studied period.  $G_a$ ,  $G_s$  and  $\Omega$  values were calculated from averaged sap flow measurements around noon (1100–1300 LT). Grey and open bars in d–i denote values calculated according to Case 1 (canopy extinction coefficient of  $k = 0.65$  for all sites) and Case 2 ( $k = 0.7$  for KR and KW and  $k = 0.3$  for SH), respectively (see text). Vertical bars represent the standard error. Different letters indicate significant differences among trees within each stand (Tukey's test;  $P < 0.05$ ).



Campbell and Norman 1998). The reported values of  $k$  vary from 0.3 to 0.7 for Japanese beech, and trees in the PAO population tend to show lower  $k$  values than those in the JAS population (Nomoto 1964, Ogawa 1967, Maruyama 1977). In practice, we obtained a  $k$  value of 0.6 for trees in the SH stand (PAO population) (T. Hiura, unpublished data). Hence, to evaluate the end-members of the mechanisms causing the  $G_S$  shift, we calculated  $G_S$  and  $\Omega$  in two different ways. First (Case 1), using only one  $k$  value ( $\approx 0.65$ ), which is considered to represent Japanese beech (Ogawa 1967). Second (Case 2), we used a  $k$  value of 0.7 for trees in the KR and KW stands (JAS population) and a  $k$  value of 0.3 for trees in the SH stand (PAO population). The value of  $k$  observed in the SH stand (0.6) was higher than that anticipated for trees in the PAO population. Therefore, the  $k$  value of 0.65 used in the Case 1 calculation is reasonable.

The relationship between  $R_n$  and  $R_s$  was calculated using only results from trees in the SH stand. Landsberg and Gower (1997) pointed out that a  $R_n/R_s$  value of 0.8 would seldom be much in error, while values of  $R_n/R_s$  varied between 0.67 and 0.91 for the various forest types. Since the calculated  $G_S$  decreases with increasing  $R_n$  (see Eq. (4)), we calculated using a  $R_n/R_s$  value of 0.9 for trees in the KR stand and a  $R_n/R_s$  value of 0.7 for trees in the KW stand, respectively. We confirmed that the values of  $G_S$  and  $\Omega$  calculated under the assumption were larger in the KR stand than in the KW and SH stands. Thus, differences in the  $R_n/R_s$  relationship among the three sites would have little effect on our conclusions.

Figure 8 shows the environmental factors  $R_s$ ,  $D$  and  $u$ , which controlled the transpiration characteristics during the study period. Although frequency distributions of  $u$  varied among the three sites, averaged  $u$  values over the study period were similar at all sites (Figure 8C). Thus, mean  $G_a$  varied in the order  $KR < KW < SH$  (ANOVA,  $P < 0.001$ ; Figure 7A–C) corresponding to the individual leaf size variation in the order  $KR > KW > SH$  (see Eq. (7) and Figure 2B).

The mean  $G_S$  of the four trees calculated using Case 1 was significantly higher in the KR stand than in the KW and SH stands, and there was no significant difference in the  $G_S$  between the KW and SH stands at  $P = 0.05$  level (ANOVA; Figure 7D–F). On the other hand, we found an inverse relationship between  $k$  and the calculated  $G_S$ . As a result, the mean  $G_S$  in Case 2 did not significantly differ among the sites (ANOVA; Figure 7D–F). However, since we used the end-member  $k$  and the  $P$ -value was marginal ( $P = 0.058$ ) in Case 2, it was possible to accept at least the order  $KR = SH > KW$ . Frequencies of high  $R_s$  ( $\geq 600 \text{ W m}^{-2}$ ) and low  $D$  ( $\leq 1.0 \text{ kPa}$ ) did not differ between the sites (Figure 8A, B), and therefore, the higher value of the mean  $G_S$  in the KR stand in Case 1 and the similarity between the KR and SH stands in Case 2 were attributed to their potential  $G_S$  ability, e.g., maximum or reference value of  $G_S$  (see Oren et al. 1999).

Consequently, calculated value of  $\Omega$  were highest for trees in the KR stand, while lower values were obtained for trees in the KW and SH stands (Figure 7G–I). This trend was

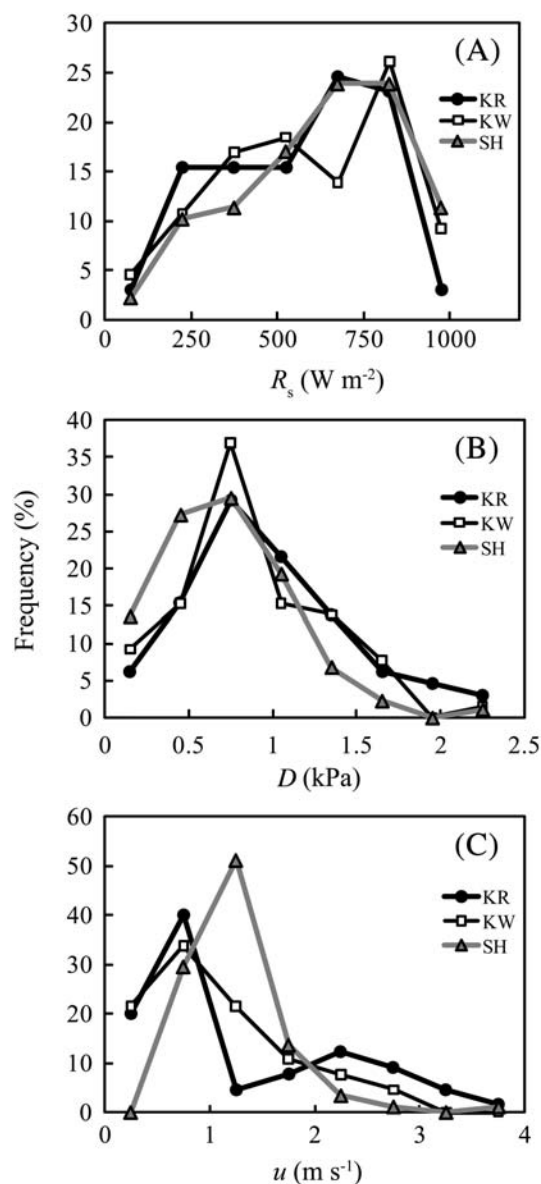


Figure 8. Frequency distribution of solar radiation ( $R_s$ ) (A), atmospheric humidity deficit ( $D$ ) (B) and wind speed ( $u$ ) (C) averaged around noon (1100–1300 LT) in the KR, KW and SH stands.

observed in values calculated using both Cases 1 and 2 (ANOVA,  $P < 0.01$  and 0.05, respectively).  $\Omega$  was  $\sim 0.45$  for the KR stand and  $\sim 0.2$  for the KW and SH stands. These are somewhat representative values that indicate the canopies' decoupling from or coupling to the atmosphere (e.g., Granier et al. 2000, Wilson and Baldocchi 2000, Wullschlegel et al. 2000). This result suggested that  $E$  of Japanese beech trees in the KW and SH stands was highly sensitive to  $G_S$  and  $D$ , similarly to conifers (Kelliher et al. 1993, Law et al. 2001, Kumagai et al. 2009). However, trees in the KR stand were more sensitive to  $R_n$  and less sensitive to  $G_S$  compared with other broad-leaved trees (Herbst 1995, Granier et al. 2000, Kumagai et al. 2004).

The relationship between  $R_n$  and  $E_L$  further reveals differences in  $E$  characteristics of Japanese beech trees among the

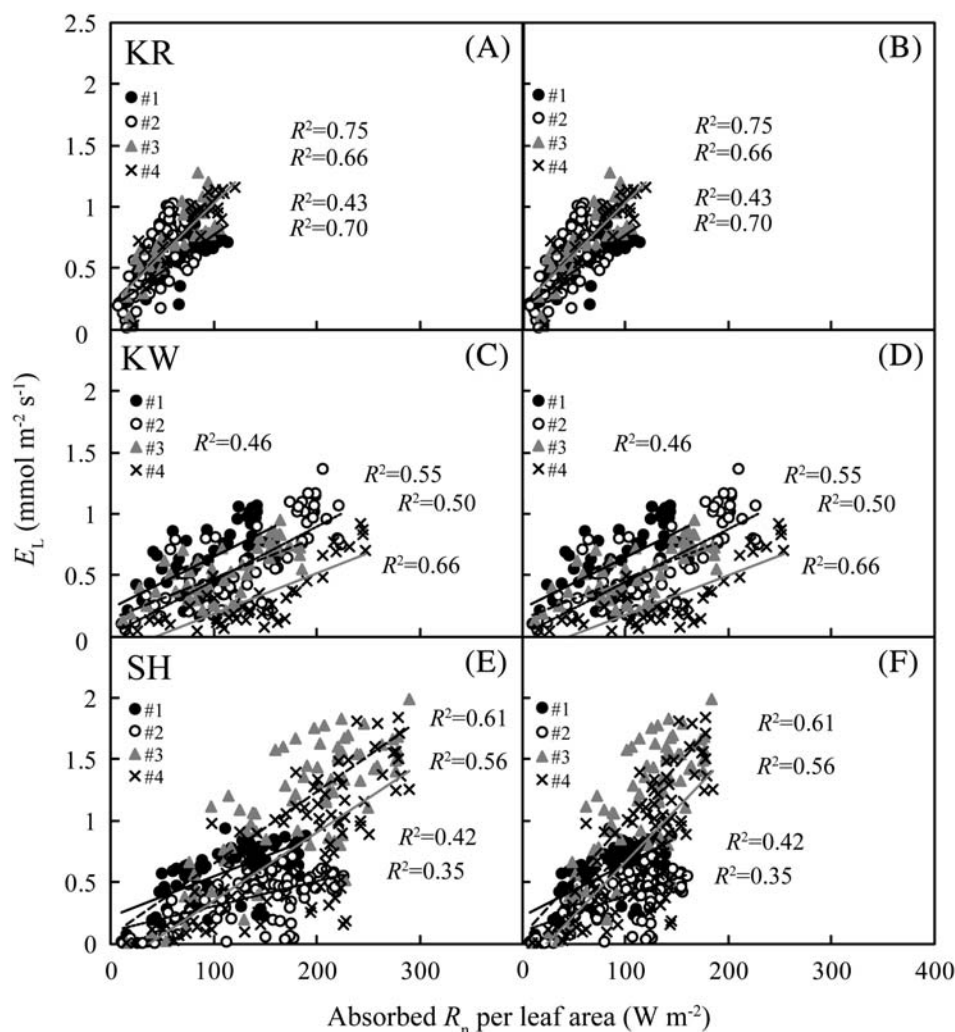


Figure 9. Relationships between absorbed net radiation ( $R_n$ ) per leaf area and tree transpiration per unit leaf area ( $E_L$ ) for each sample tree in the KR (A, B), KW (C, D) and SH stands (E, F). Values were calculated according to Case 1 (A, C, E) and Case 2 (B, D, F). Values represent averaged measurements obtained around noon (1100–1300 LT). Lines represent linear regression of data from each sample tree.

three sites (Figure 9). On average, this relationship explained a greater percentage of the observed variation in  $E_L$  in the KR stand ( $R^2 = 0.43$ – $0.75$ ) than in the KW ( $R^2 = 0.46$ – $0.66$ ) and SH ( $R^2 = 0.35$ – $0.61$ ) stands, as expected by the higher value of  $\Omega$  in the KR stand (see Kumagai et al. 2004). The differences in individual leaf size (Figure 2B) and crown shape (Figure 3A) among the three sites generated the variation in the  $R_n$  absorbed per leaf area in the order  $KR < KW < SH$ . Using Case 1, this result in higher values of slope in the KR stand ( $6.0 \times 10^{-3}$ – $8.6 \times 10^{-3}$ ) than in the KW ( $3.3 \times 10^{-3}$ – $4.4 \times 10^{-3}$ ) and SH ( $2.1 \times 10^{-3}$ – $5.8 \times 10^{-3}$ ) stands (Figure 9A, C, E). In Case 2, a lower  $k$  value in the SH stand results in a higher slope value ( $2.9 \times 10^{-3}$ – $9.2 \times 10^{-3}$ ) (Figure 9B, D, F). It is important to note that these higher values of slope were accompanied by higher  $G_S$  values. Maintaining higher  $G_S$  would confer a carbon uptake advantage upon the tree species, but the cost to the species would be extra water loss. Hence, we hypothesized that the trees with higher  $G_S$  in the KR stand in Case 1 (Figure 7D) and in the KR and SH stands in Case 2 (Figure 7D, F) had to decrease  $E$

by reducing absorbed  $R_n$  per leaf area. This could be achieved by adjusting the individual leaf size and crown shape (for KR; Figure 9B) and adjusting light attenuation within the crown (for SH; Figure 9F).

Bayramzadeh et al. (2008) examined differences in vessel element anatomy relating to xylem conductivity and physiological and morphological characteristics of leaves in Japanese beech seedlings. The seedlings were obtained from seven sources and were grown at a single site. They found geographical variations in the xylem conductivity and showed that the transpiration rate/stomatal conductance was positively correlated with theoretical hydraulic conductance in the xylem. However, their results did not show a distinct cline, e.g., between JAS and PAO populations, in these  $E$  characteristics. The JAS trees (Clade I) receive abundant water from snowmelt at the timing of leaf expansion, whereas PAO trees (Clade II + III) are often exposed to drought conditions (see Figure 1). This environmental difference could affect the difference in leaf area, leaf thickness and stomata compartment size of the heterobaric leaves between the JAS

and PAO populations (Koike 2008). In particular, the smaller compartment of heterobaric leaves in the PAO can control the sensitivity of  $G_S$  to drought. The architecture of these leaves is adapted to prevent excessive cavitation and thus results in smaller  $G_S$  (e.g., Terashima 1992). Therefore, provided that Case 1 is reasonable, the higher  $G_S$  in the KR stand and lower  $G_S$  in the SH stand can be attributed to genotypic variation, that is, trees in the KR and SH stands belong to Clade I and III, respectively (see Yamazaki et al. 2007). Here, we should note that the  $G_S$  in the KW stand was smaller than that in the KR stand and almost the same as that in the SH stand (Figure 7D, E, F) although trees in the KR and KW stands belong to Clade I. In fact, leaf thickness and area differed between the KR and KW stands. Thus, we suggest that there could be a phenotypic variation in the  $E$  characteristics between the KR and KW stands (see Abrams 1994, Addington et al. 2006).

It is interesting to focus on the smaller  $G_S$  in SH calculated using a  $k$  value of 0.65 because, although the SH trees in the PAO population (Clade III) are adapted to dry conditions, they receive considerable precipitation and have a low atmospheric demand for evaporation (see Figure 8B). The Japanese beech trees in Kyushu Island (see Figure 1) are thought to represent a refuge PAO population that was confined to mountain altitudes during and after the last glacial period (Tomaru 2008). Thus, we presume that the SH trees still retain typical PAO type (Clade III)  $E$  characteristics.

## Conclusions

We conducted biometric and  $F_d$  measurements in trees located in three different Japanese beech stands across the Japanese archipelago to examine the differences in  $E$  characteristics. On the basis of our data and previously reported data on geographical variation in chloroplast DNA of Japanese beech (Figure 1; Fujii et al. 2002), we found that genotypic and phenotypic variations control the  $E$  of Japanese beech trees. These variations included the magnitude of  $G_S$ , adjustment of available radiation energy per leaf area via changes in crown shape and individual leaf size and, possibly, changes that effect light attenuation within the crown. We thoroughly investigated and evaluated the  $E$  of whole 'adult' trees using measurements for circumferential and radial variations in  $F_d$  in the stem. These measurements provided extensive data, despite the fact that we measured only four sample trees for each plot at the three study stands (see Table 1). These results allow us to consider the influence of genotypic and phenotypic variation in the characteristics of plant species over their geographical range and how these variations affect their growth performance. While further study at additional stands and using greater sample sizes is required, understanding these variations is the first step to determining how such changes affect the global forest ecosystem's water and carbon cycling (see Berninger and Nikinmaa 1997, Poyatos et al. 2007).

## Acknowledgments

This work was supported by Grants-in-Aid for Scientific Research (nos. 19380079, 20380090 and 21248017) from the Ministry of Education, Science and Culture, Japan. We thank Masahiro Nakamura and Ryosuke Nomura for their assistance with site maintenance and the staff at the Field Science Center of Tohoku University and the Shiiba Research Forest of Kyushu University for providing logistical support. We would also like to thank Onno Muller, Hikaru Komatsu and Yoshiyuki Miyazawa for their helpful comments and Chris Wood for his help in English editing.

## References

- Abrams, M.D. 1994. Genotypic and phenotypic variation as stress adaptations in temperate tree species: a review of several case studies. *Tree Physiol.* 14:833–842.
- Addington, R.N., L.A. Donovan, R.J. Mitchell, J.M. Vose, S.D. Pecot, S.B. Jack, U.G. Hacke, J.S. Sperry and R. Oren. 2006. Adjustments in hydraulic architecture of *Pinus palustris* maintain similar stomatal conductance in xeric and mesic habitats. *Plant Cell Environ.* 29:535–545.
- Bayramzadeh, V., R. Funada and T. Kubo. 2008. Relationship between vessel element anatomy and physiological as well as morphological traits of leaves in *Fagus crenata* seedlings originated from different provenances. *Trees* 22:217–224.
- Berninger, F. 1997. Effects of drought and phenology on GPP in *Pinus sylvestris*: a simulation study along a geographical gradient. *Funct. Ecol.* 11:33–42.
- Berninger, F. and E. Nikinmaa. 1997. Implications of varying pipe model relationships on Scots pine growth in different climates. *Funct. Ecol.* 11:146–156.
- Campbell, G.S. and J.M. Norman. 1998. An introduction to environmental biophysics 2nd edn. Springer, New York, 286 p.
- Choudhury, B.J. and J.L. Monteith. 1988. A four-layer model for the heat budget of homogeneous land surfaces. *Q. J. R. Meteorol. Soc.* 114:373–398.
- Cienciala, E., J. Kučera and A. Malmer. 2000. Tree sap flow and stand transpiration of two *Acacia mangium* plantations in Sabah, Borneo. *J. Hydrol.* 236:109–120.
- DeLucia, E.H., H. Maherali and E.V. Carey. 2000. Climate-driven changes in biomass allocation in pines. *Glob. Chang. Biol.* 6:587–593.
- Delzon, S., M. Sartore, A. Granier and D. Loustau. 2004. Radial profiles of sap flow with increasing tree size in maritime pine. *Tree Physiol.* 24:1285–1293.
- Ford, C.R., C.E. Goranson, R.J. Mitchell, R.E. Will and R.O. Teskey. 2005. Modeling canopy transpiration using time series analysis: a case study illustrating the effect of soil moisture deficit on *Pinus taeda*. *Agric. For. Meteorol.* 130:163–175.
- Fujii, N., N. Tomaru, K. Okuyama, T. Koike, T. Mikami and K. Ueda. 2002. Chloroplast DNA phylogeography of *Fagus crenata* (Fagaceae) in Japan. *Plant Syst. Evol.* 232:21–33.
- Granier, A. 1987. Evaluation of transpiration in a Douglas-fir stand by means of sap flow measurements. *Tree Physiol.* 3:309–320.
- Granier, A. and D. Loustau. 1994. Measuring and modeling the transpiration of a maritime pine canopy from sap-flow data. *Agric. For. Meteorol.* 71:61–81.
- Granier, A., P. Biron and D. Lemoine. 2000. Water balance, transpiration and canopy conductance in two beech stands. *Agric. For. Meteorol.* 100:291–308.
- Hacke, U.G., J.S. Sperry, B.E. Ewers, D.S. Ellsworth, K.V.R. Schäfer and R. Oren. 2000. Influence of soil porosity on water use in *Pinus taeda*. *Oecologia* 124:495–505.

- Hagiwara, S. 1977. A cline on leaf size of beech *Fagus crenata*. *Shuseibutsugaku-kenkyu* 1:39–51 (in Japanese)
- Herbst, M. 1995. Stomatal behavior in a beech canopy: an analysis of Bowen ratio measurements compared with porometer data. *Plant Cell Environ.* 18:1010–1018.
- Herbst, M., P.T.W. Rosier, M.D. Morecroft and D.J. Gowing. 2008. Comparative measurements of transpiration and canopy conductance in two mixed deciduous woodlands differing in structure and species composition. *Tree Physiol.* 28:959–970.
- Hirose, S., A. Kume, S. Takeuchi, Y. Utsumi, K. Otsuki and S. Ogawa. 2005. Stem water transport of *Lithocarpus edulis*, an evergreen oak with radial-porous wood. *Tree Physiol.* 25:221–228.
- Hiura, T. 1996. Geographic variation and maintenance of species diversity of beech forests in Japan. *Jpn. J. Ecol.* 46:175–178 (in Japanese)
- Hiura, T. 1998. Shoot dynamics and architecture of saplings in *Fagus crenata* across its geographical range. *Trees* 12:274–280.
- Horikawa, Y. 1972. Atlas of the Japanese flora. Gakken Co., Tokyo, p 862 (in Japanese)
- Iio, A., H. Fukasawa, Y. Nose, S. Kato and Y. Kakubari. 2005. Vertical, horizontal and azimuthal variations in leaf photosynthetic characteristics within a *Fagus crenata* crown in relation to light acclimation. *Tree Physiol.* 25:533–544.
- Jarvis, P.G. and K.G. McNaughton. 1986. Stomatal control of transpiration: scaling up from leaf to region. *Adv. Ecol. Res.* 15:1–49.
- Jones, H.G. 1992. Plants and microclimate: a quantitative approach to environmental plant physiology 2nd edn. Cambridge University Press, Cambridge, p 428.
- Kelliher, F.M., R. Leuning and E.-D. Schulze. 1993. Evaporation and canopy characteristics of coniferous forests and grasslands. *Oecologia* 95:153–163.
- Koike, T. 2008. Geographical variation in ecophysiological response of Japanese beech tree to environment—photosynthetic function and leaf morphology and structure. In *Applied Ecology for Restoration of Beech Forests*. Eds. K. Terazawa and H. Koyama. Bun-ichi Sogo Shyuppan, Tokyo, p 213–233 (in Japanese)
- Koike, T. and Y. Maruyama. 1998. Comparative ecophysiology of the leaf photosynthetic traits in Japanese beech grown in provenances facing the Pacific Ocean and the Sea of Japan. *J. Phyto-geogr. Taxon.* 46:23–28 (in Japanese)
- Köstner, B.M.M., E.-D. Schulze, F.M. Kelliher, D.Y. Hollinger, J.N. Byers, J.E. Hunt, T.M. McSeveny, R. Meserth and P.L. Weir. 1992. Transpiration and canopy conductance in a pristine broad-leaved forest of *Nothofagus*: an analysis of xylem sap flow and eddy correlation measurements. *Oecologia* 91:350–359.
- Köstner, B., P. Biron, R. Siegwolf and A. Granier. 1996. Estimates of water vapor flux and canopy conductance of Scots pine at the tree level utilizing different xylem sap flow methods. *Theor. Appl. Climatol.* 53:105–113.
- Kubota, M., J. Tenhunen, R. Zimmermann, M. Schmidt, S. Adiku and Y. Kakubari. 2005. Influences of environmental factors on the radial profile of sap flux density in *Fagus crenata* growing at different elevations in the Naeba Mountains, Japan. *Tree Physiol.* 25:545–556.
- Kumagai, T. 2001. Modeling water transportation and storage in sapwood—model development and validation. *Agric. For. Meteorol.* 109:105–115.
- Kumagai, T., T.M. Saitoh, Y. Sato, T. Morooka, O.J. Manfroi, K. Kuraji and M. Suzuki. 2004. Transpiration, canopy conductance and the decoupling coefficient of a lowland mixed dipterocarp forest in Sarawak, Borneo: dry spell effects. *J. Hydrol.* 287:237–251.
- Kumagai, T., T.M. Saitoh, Y. Sato, H. Takahashi, O.J. Manfroi, T. Morooka, K. Kuraji, M. Suzuki, T. Yasunari and H. Komatsu. 2005. Annual water balance and seasonality of evapotranspiration in a Bornean tropical rainforest. *Agric. For. Meteorol.* 128:81–92.
- Kumagai, T., S. Aoki, K. Otsuki and Y. Utsumi. 2009. Impact of stem water storage on diurnal estimates of whole-tree transpiration and canopy conductance from sap flow measurements in Japanese cedar and Japanese cypress trees. *Hydrol. Process.* 23:2335–2344.
- Kutsch, W. L., M. Herbst, R. Vanselow, P. Hummelshøj, N.O. Jensen and L. Kappen. 2001. Stomatal acclimation influences water and carbon fluxes of a beech canopy in northern Germany. *Basic Appl. Ecol.* 2:265–281.
- Kuuluvainen, T. 1992. Tree architectures adapted to efficient light utilization: is there a basis for latitudinal gradients? *Oikos* 65:275–284.
- Landsberg, J.J. and S.T. Gower. 1997. Applications of physiological ecology to forest management. Academic Press, San Diego, p 66–67.
- Law, B.E., A.H. Goldstein, P.M. Anthoni, M.H. Unsworth, J.A. Panek, M.R. Bauer, J.M. Francheboud and N. Hultman. 2001. Carbon dioxide and water vapor exchange by young and old ponderosa pine ecosystems during a dry summer. *Tree Physiol.* 21:299–308.
- Lu, P., W.J. Müller and E.K. Chacko. 2000. Spatial variations in xylem sap flux density in the trunk of orchard-grown, mature mango trees under changing soil water conditions. *Tree Physiol.* 20:683–692.
- Lu, P., L. Urban and P. Zhao. 2004. Granier's thermal dissipation probe (TDP) method for measuring sap flow in trees: theory and practice. *Acta Bot. Sin.* 46:631–646.
- Magnani, F., S. Leonardi, R. Tognetti, J. Grace and M. Borghetti. 1998. Modelling the surface conductance of a broad-leaf canopy: effects of partial decoupling from the atmosphere. *Plant Cell Environ.* 21:867–879.
- Martin, T.A., K.J. Brown, J. Cermak, R. Ceulemans, J. Kucera, F.C. Meinzer, J.S. Rombold, D.G. Sprugel and T.M. Hinckley. 1997. Crown conductance and tree and stand transpiration in a second-growth *Abies amabilis* forest. *Can. J. For. Res.* 27:797–808.
- Maruyama, K. 1977. Beech forest in the Naeba Mountains, part I. Comparison of forest structure, biomass and net productivity between the upper and lower parts of beech forest zone. In *Primary Productivity of Japanese Forests, JIBP Synthesis*. Eds. T. Shidei and T. Kira 16. University of Tokyo Press, Tokyo, p 186–201.
- Matsui, T., T. Yagihashi, T. Nakaya, N. Tanaka and H. Taoda. 2004. Climatic controls on distribution of *Fagus crenata* forests in Japan. *J. Veg. Sci.* 15:57–66.
- Meinzer, F.C., S.A. James, G. Goldstein and D. Woodruff. 2003. Whole-tree water transport scales with sapwood capacitance in tropical forest canopy trees. *Plant Cell Environ.* 26:1147–1155.
- Nomoto, N. 1964. Primary productivity of beech forest in Japan. *Jpn. J. Bot.* 18:385–421.
- Ogawa, H. 1967. Three-dimensional structure of Ashiu beech forest in relation to light distribution. In *Studies on the Methods for Assessing Primary Production of Forests, Progress Report of JIBP/PT for 1966*. Ed. T. Kira 45–52 (in Japanese)
- Oren, R., J.S. Sperry, G.G. Katul, D.E. Pataki, B.E. Ewers, N. Phillips and K.V.R. Schäfer. 1999. Survey and synthesis of intra- and interspecific variation in stomatal sensitivity to vapour pressure deficit. *Plant Cell Environ.* 22:1515–1526.
- Parkhurst, D.F. and O.L. Loucks. 1972. Optimal leaf size in relation to environment. *J. Ecol.* 60:505–537.

- Pataki, D.E. and R. Oren. 2003. Species differences in stomatal control of water loss at the canopy scale in a mature bottomland deciduous forest. *Adv. Water Resour.* 26:1267–1278.
- Phillips, N., A. Nagchaudhuri, R. Oren and G. Katul. 1997. Time constant for water transport in loblolly pine trees estimated from time series of evaporative demand and stem sapflow. *Trees* 11:412–419.
- Poyatos, R., J. Martínez-Vilalta, J. Čermák et al. 2007. Plasticity in hydraulic architecture of Scots pine across Eurasia. *Oecologia* 153:245–259.
- Tateishi, M., T. Kumagai, Y. Utsumi, T. Umebayashi, Y. Shiiba, K. Inoue, K. Kaji, K. Cho and K. Otsuki. 2008. Spatial variations in xylem sap flux density in evergreen oak trees with radial-porous wood: comparisons with anatomical observations. *Trees* 22:23–30.
- Terazawa, K. and H. Koyama. (Eds). *Applied ecology for restoration of beech forests*. Bun-ichi Sogo Shuppan Co., Tokyo, p 310 (in Japanese).
- Terashima, I. 1992. Anatomy of non-uniform leaf photosynthesis. *Photosyn. Res.* 31:195–212.
- Tomaru, N., T. Mitsutsuji, M. Takahashi, Y. Tsumura, K. Uchida and K. Ohba. 1997. Genetic diversity in Japanese beech, *Fagus crenata*: influence of the distributional shift during the late-Quaternary. *Heredity* 78:241–251.
- Tomaru, N. 2008. Genetic variation and structure of Japanese beech population—the effect of historical geological shift on the distribution. In *Applied Ecology for Restoration of Beech Forests*. Eds. K. Terazawa and H. Koyama Bun-ichi Sogo Shyuppan, Tokyo, p 187–212 (in Japanese)
- Uemura, A., A. Ishida, T. Nakano, I. Terashima, H. Tanabe and Y. Matsumoto. 2000. Acclimation of leaf characteristics of *Fagus* species to previous-year and current-year solar irradiances. *Tree Physiol.* 20:945–951.
- Uemura, A., A. Ishida, D.J. Tobias, N. Koike and Y. Matsumoto. 2004. Linkage between seasonal gas exchange and hydraulic acclimation in the top canopy leaves of *Fagus* trees in a mesic forest in Japan. *Trees* 18:452–459.
- Uemura, A., A. Ishida and Y. Matsumoto. 2005. Simulated seasonal changes of CO<sub>2</sub> and H<sub>2</sub>O exchange at the top canopies of two *Fagus* trees in a winter-deciduous forest, Japan. *For. Ecol. Manag.* 212:230–242.
- Wilson, K.B. and D.D. Baldocchi. 2000. Seasonal and interannual variability of energy fluxes over a broadleaved temperate deciduous forest in North America. *Agric. For. Meteorol.* 100:1–18.
- Wullschleger, S.D. and A.W. King. 2000. Radial variation in sap velocity as a function of stem diameter and sapwood thickness in yellow-poplar trees. *Tree Physiol.* 20:511–518.
- Wullschleger, S.D., K.B. Wilson and P.J. Hanson. 2000. Environmental control of whole-plant transpiration, canopy conductance and estimates of the decoupling coefficient for large red maple trees. *Agric. For. Meteorol.* 104:157–168.
- Yamazaki, J., E. Yoda, A. Takahashi, K. Sonoike and E. Maruta. 2007. Pacific Ocean and Japan Sea ecotypes of Japanese beech (*Fagus crenata*) differ in photosystem responses to continuous high light. *Tree Physiol.* 27:961–968.
- Zang, D., C.L. Beadle and D.A. White. 1996. Variation of sapflow velocity in *Eucalyptus globulus* with position in sapwood and use of a correction coefficient. *Tree Physiol.* 16:697–703.